Korean J. Chem. Eng., 32(10), 2161-2167 (2015)
DOI: 10.1007/s11814-015-0150-7

pISSN: 0256-1115
eISSN: 1975-7220

Removal characteristics of Cd(II) ions from aqueous solution on ordered mesoporous carbon

Linhang Lu, Haibo Zhao, Lu Yan, Guowei Wang, Yulin Mao, Xin Wang, Kai Liu, Xiufang Liu, Qian Zhao†, and Tingshun Jiang

School of Chemistry and Chemical Engineering, Jiangsu University, Zhenjiang 212013, Jiangsu, China
(*Received 28 January 2015 • accepted 10 July 2015*)

Abstract−Ordered mesoporous carbon (CMK-3) was synthesized using SBA-15 mesoporous molecular sieve as a template and sucrose as carbon source. The materials were characterized by XRD, TEM and N_2 physical adsorption technique. The resulting CMK-3 was used as adsorbent to remove Cd(II) ions from aqueous solution. The effect of pH, contact time and temperature on adsorption process was investigated in batch experiments. The results showed that the removal percentage could reach *ca.* 90% at the conditions of initial Cd(II) ions concentration of 20 mg/L, dose of 20 mg, pH 6.5, contact time of 3 h and 293 K. Langmuir and Freundlich models were employed to describe the adsorption equilibrium. The kinetics data were described by the pseudo-first-order and pseudo-second-order models, respectively. The adsorption isotherm was well fitted to the Langmuir model, and the adsorption process was well described by the pseudo-second-order kinetic model.

Keywords: Mesoporous Carbon, Adsorption, Cd(II) Ions, Kinetics

INTRODUCTION

With modern industrial development, water pollution caused by heavy metal ions has been a major environmental issue due to their toxic effect to human health and other organisms [1-3]. Generally, metal-bearing effluents originate from metal plating, mining operation, nuclear power plant, metallurgical industries, tanneries and battery manufacturing industries, and they contain various toxic heavy metals such as lead, cobalt, nickel, cadmium, chromium and mercury. Among these, cadmium has received considerable attention owing to its high toxicity, non-biodegradability and long half-life. It accumulates slowly in the body of living creatures by the food chain, and even small concentration can cause serious damage to kidney and bone [4]. Consequently, it is necessary to remove or decrease the amount of heavy metals to acceptable level.

The conventional strategies for removal of heavy metal ions from aqueous media such as chemical precipitation [5], coagulation and flocculation [6], ion exchange [7], evaporation, reverse osmosis [8], co-precipitation, oxidation [9], electrodialysis [10] and adsorption [11] have been successfully applied. However, most of them have some disadvantages such as secondary pollution and inefficiency. Among various available treatment technologies, adsorption is highly popular and has been widely practiced in industrial wastewater treatment due to its high efficiency, convenience, fast response and low price [12,13].

Various materials such as zeolites, silica gel, clay minerals, polymeric materials, and iron oxide nanomaterials have been used as adsorbents for removal of pollutants from wastewater [14-16]. Recently, much attention has been paid to carbonaceous materials such as activated carbon, carbon nanotubes and graphene oxide [17-20] due to their thermal and chemical stabilities. Among these, activated carbon is the most popular and is widely used in water pollution control owing to its pore structure with a large surface area ranging from 600-2,000 m^2/g [21,22]. In spite of extensive uses of activated carbon, its application has been sometimes limited due to the dominance of micropores (<2 nm) in its pore structure [23]. Compared with activated carbon, mesoporous materials are considered to be promising adsorbents for removal of heavy metal ions owing to their unique pore structures, high surface areas and tunable pore diameters [24].

Mesoporous carbon, a member of carbon materials family, was discovered in 1999 [25]. Due to its high surface area, large pore volume, ordered pore structure and mechanical stability [26], ordered mesoporous carbon is considered to be an attractive adsorbent and has proved to be a kind of efficient adsorbent for removal of environmental contaminants [27] and adsorption of biomolecules [28]. However, most of the previous reports aimed at investigating the removal of organic compound from aqueous solution onto ordered mesoporous carbon, seldom was attention paid to the study of removal of heavy metal ions.

The main objective of present work was to synthesize ordered mesoporous carbon by hard template method and characterize it by a variety of physicochemical techniques, to evaluate its adsorption capacity using Cd(II) ions as a target pollutant, to investigate the effect of dose, contact time, temperature and pH on Cd(II) ions adsorption, and to discuss the behavior of Cd (II) ion adsorption

†To whom correspondence should be addressed.
E-mail: qianzhao@ujs.edu.cn

with kinetics and isotherm models.

EXPERIMENTAL

1. Materials

Concentrated sulfuric acid, hydrochloric acid, hydrofluoric acid, sucrose, tetraethyl orthosilicate (TEOS, 98%) and cadmium chloride ($CdCl_2 \cdot 3/2H_2O$) were obtained from Shanghai Chemical Reagent Corporation, PR China. Triblockcopolymer Pluronic P123 ($EO_{20}PO_{70}EO_{20}$, Mw=5800) was from Sigma-Aldrich. All the reagents were analytical grade. SBA-15 was prepared using P123 as a template and tetraethyl orthosilicate as silicon source [29].

2. Synthesis of Mesoporous Carbon (CMK-3)

The mesoporous carbon was synthesized by hard template method using mesoporous SBA-15 as a template and sucrose as carbon source according to the Ref. [30]. 1 g of SBA-15 powder was mixed with an aqueous solution consisting of 1.25 g sucrose, 0.14 g of H_2SO_4 and 5.0 g of deionized H_2O. The resulting mixture was placed into an oven for 6 h at 100 °C and then the oven was heated to 160 °C and kept the temperature for 6 h. The obtained dark brown sample was milled. Subsequently, 0.75 g of sucrose, 0.1 g of H_2SO_4 and 5.0 g of deionized H_2O were added into the milled sample with stirring uniformly. After the above same heating treatment, the resultant sample was placed in a tubular furnace and the tubular furnace was heated from room temperature to 900 °C at a heating rate of 5 °C/min in a flow of N_2 and kept at the temperature for 3 h. To remove the silica template, the carbonized composite obtained after pyrolysis was washed with 5 wt% hydrofluoric acid. The resulting sample was filtered, washed with deionized water and dried at 120 °C, denoted as CMK-3.

3. Characterization

The XRD patterns of samples were recorded on a Rigaku D/MAX 2500PC powder XRD instrument with Cu Kα radiation (λ=0.15418 nm) at 40 kV and 50 mA, the scanning range is 0.5~8° and the scanning speed 1°/min. Transmission electron microscopy (TEM) morphologies of samples were observed on a Philips TEMCNAI-12 with an acceleration voltage of 200 kV. Specific surface areas were measured by using a NOVA2000e analytical system made by Quantachrome Corporation (USA). The specific surface areas were calculated by BET method. The pore size distribution and pore volume were calculated by BJH method.

4. pH Point of Zero Charge (pH_{zpc})

Measurement of the adsorbent ZPC was carried out according to the Ref. [31]. 0.1 mol/L KCl solution was prepared and its initial pH was adjusted from 2 to 12 by using NaOH and HCl. Then, 50 mL of 0.1 mol/L KCl solution was taken in the 100 mL flasks and 0.02 g (20 mg) of CMK-3 was added to each solution, respectively. These flasks were kept for 24 h, and the final pH of the solution was measured by using a pH meter and plotted against the initial pH. The pH at which the curve crosses the $pH_{initial}$=pH_{final} line was taken as pH_{zpc}.

5. Adsorption Experiment

Adsorption experiments of Cd(II) ions on CMK-3 were according to the batch method. The effect of pH, contact time, and temperature on adsorption of Cd(II) ions was investigated. In a reaction mixture, 20 mg of CMK-3 was added into 50 mL of Cd(II) ions solution at concentration range from 8 to 20 mg/L with a magnetic stirring at room temperature in a conical flask. The pH of solution was 2, 4, 6.5 and 8, respectively. After a period of time, the suspension was centrifugation at 6,000 rpm for 10 min. The liquid phase was separated and the cadmium ions concentration was determined by a TAS-986 atomic adsorption spectrometer (AAS) made by Beijing Purkinje General Instrument Co., Ltd. (China).

6. Removal Percentage and Adsorption Capacity

The removal percentage of Cd(II) ions (θ) and the adsorption amount of Cd(II) ions on CMK-3 at time t (q_t, mg/g), were calculated by the following equations:

$$\theta = \frac{C_0 - C_t}{C_0} \times 100\% \quad (1)$$

$$q_t = \frac{C_0 - C_t}{m} \times V \quad (2)$$

where C_0 (mg/L) stands for the initial concentration of Cd(II) ions; C_t (mg/L) is the concentration of Cd(II) ions at time t; V (L) is the volume of the solution; m (g) is the mass of the adsorbent.

7. Adsorption Isotherm

Langmuir and Freundlich isotherms are used in experiment to describe the adsorption behavior of Cd(II) ions on CMK-3. The linear forms of the Langmuir and Freundlich models are expressed by the following equations:

$$\frac{1}{q_e} = \frac{1}{q_m} + \frac{1}{K_L q_m C_e} \quad (3)$$

$$\ln q_e = \ln K_F + \frac{1}{n} \ln C_e \quad (4)$$

where C_e is the equilibrium concentration of Cd(II) ions in aqueous solution (mg/L); q_e (mg/g) is the adsorption amount at equilibrium (mg/g); q_m is the maximum adsorption capacity of the adsorbent; K_L is Langmuir constant, K_F and n represent the Freundlich constants related to the adsorption capacity and adsorption intensity.

8. Adsorption Kinetic

The adsorption kinetic of Cd(II) ions was carried out *via* using pseudo-first-order and pseudo-second-order rate equations, respectively. The pseudo-first-order and pseudo-second-order equations are as follows:

$$\ln(q_e - q_t) = \ln q_e - k_1 t \quad (5)$$

$$\frac{t}{q_t} = \frac{1}{k_2 q_e^2} + \frac{t}{q_e} \quad (6)$$

where k_1 (min^{-1}) and k_2 (g $mg^{-1}min^{-1}$) are the rate constant of the pseudo-first-order and the pseudo-second-order adsorption; q_e and q_t represent the removed amount of Cd(II) ions at equilibrium and at time t, respectively.

Activation energy (Ea, kJ/mol) was calculated by Arrhenius equation as follows:

$$\ln k = -\frac{Ea}{RT} + \ln A \quad (7)$$

where k (g $mg^{-1}min^{-1}$) is the rate constant of the pseudo-second-

order; R is the ideal gas constant (8.314 J/mol·K); T is the absolute temperature (K); A is pre-exponential factor.

RESULTS AND DISCUSSION

1. XRD Analysis

Fig. 1 depicts the low angle XRD patterns of SBA-15 and CMK-3 samples. As displyed in Fig. 1(a), SBA-15 sample exhibits three diffraction peaks at 2θ values of 0.9°, 1.46° and 1.69°, which can be assigned to (100), (110) and (200) reflections associated with *p*6mm hexagonal symmetry [32]. Notably, we can observe that the CMK-3 sample gave a strong diffraction peak at 1.07° and two weak peaks at 1.74° and 2.1° (Fig. 1(b)), suggesting that the ordered arrangement mesoporous carbon was successfully synthesized; similar result was reported in Ref. [33]. However, the intensities of all diffraction peaks for the CMK-3 sample were lower than that of SBA-15 sample, and the positions of all reflections shifted to the higher 2θ value.

2. Nitrogen Physical Adsorption

The N_2 adsorption-desorption isotherms of SBA-15 and CMK-3 samples are given in Fig. 2. According to IUPAC classification, the N_2 adsorption-desorption isotherms of two samples are typical IV isotherm, indicating that the two samples had a mesoporous structure [34]. Also, the isotherms of the two samples exhibit a hysteresis loop, owing to capillary condensation in mesopores [26]. Furthermore, a sharp peak can be observed from the inserted pore

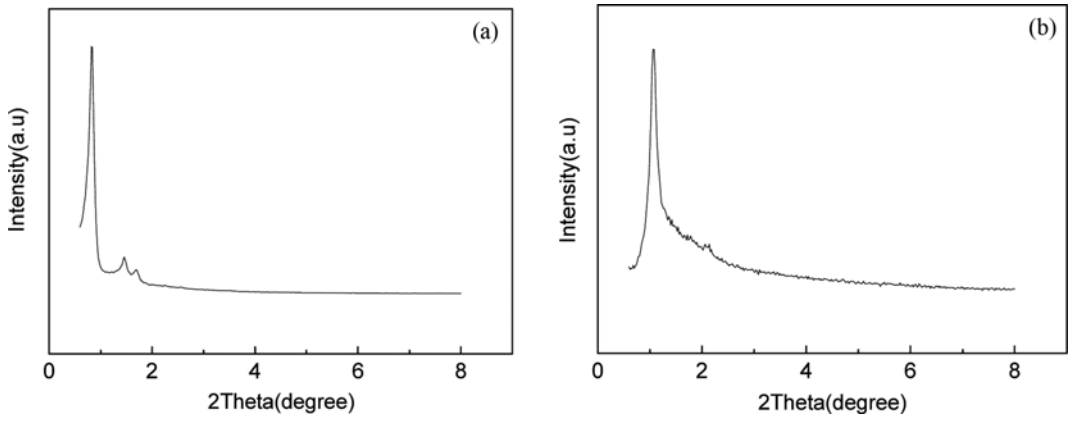

Fig. 1. XRD patterns of SBA-15 and CMK-3 samples.

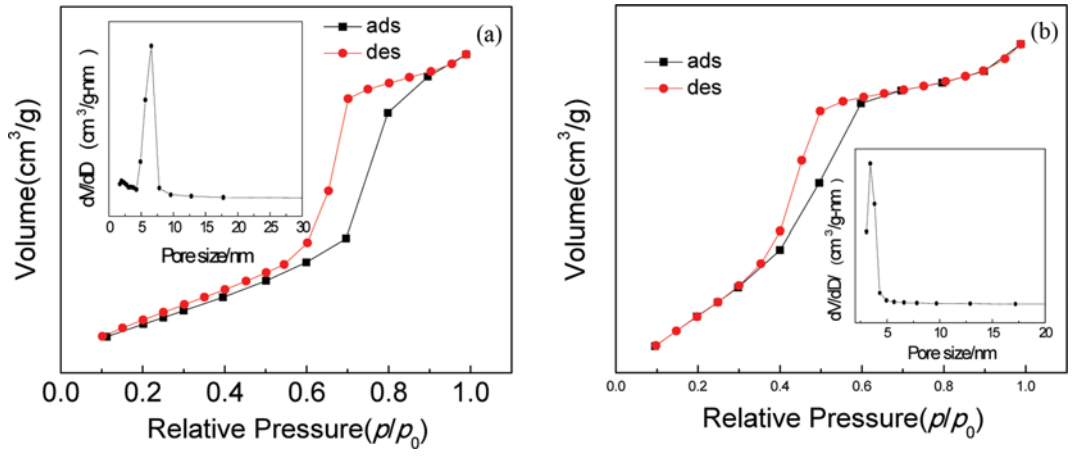

Fig. 2. Nitrogen adsorption-desorption isotherms of samples (a) SBA-15; (b) CMK-3. Inset: BJH pore size distribution calculated from the desorption branch of the isotherm.

Table 1. Surface areas, average pore sizes, total pore volumes and XRD analysis of samples

Sample	Surface area (m^2/g)	Average pore size[a] (nm)	Total pore volume (m^3/g)	$d_{(100)}$[b] (nm)	a_0[b] (nm)	t[c] (nm)
SBA-15	846	6.59	0.51	9.82	11.34	4.75
CMK-3	1036	3.43	0.85	8.26	9.54	6.11

[a]Values obtained from N_2 adsorption results
[b]Values obtained from XRD studies
[c]Wall thickness=unit cell parameter (a_0)-pore size (D)

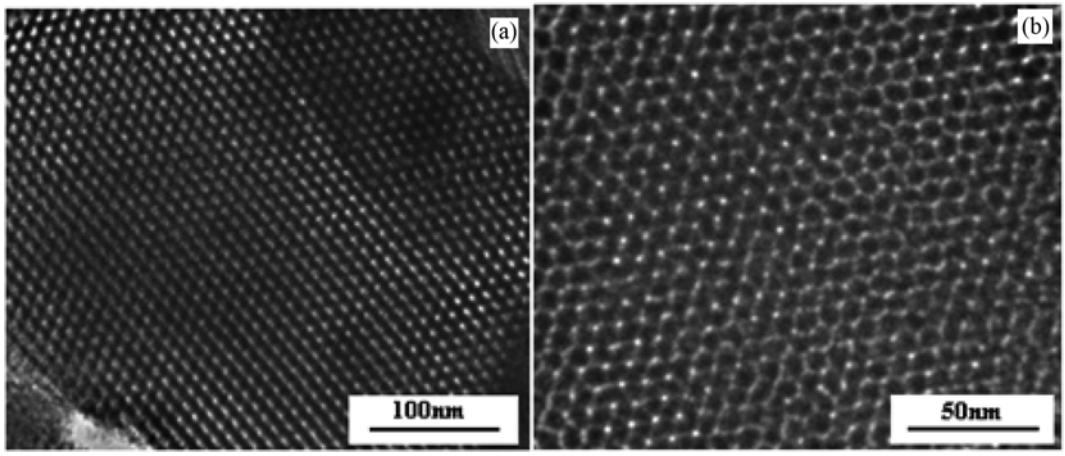

Fig. 3. TEM images of sample. (a) SBA-15; (b) CMK-3 (before Cd(II) ions adsorption).

size distribution curves, suggesting that the resulting samples have good mesoporous ordering.

Table 1 lists the textural properties of the samples. The S_{BET} of the SBA-15 and CMK-3 samples was 846 and 1,036 m^2/g and the pore size was *ca.* 6.6 and 3.4 nm, respectively. Compared with the SBA-15, the surface area increased and the pore size decreased for the CMK-3 sample, which was probably due to the structural shrinkage during the carbonization process. Similar phenomenon was in good agreement with the Ref. [30].

3. TEM Analysis

The TEM images of SBA-15 and CMK-3 samples are shown in Fig. 3. Clearly, the SBA-15 and CMK-3 samples both exhibit uniform channel arrays and well-ordered hexagonal arrangement, suggesting that two samples have the obvious mesoporous structure and good mesoporous ordering. Moreover, we observed from Fig. 3(b) that the pore size of the CMK-3 sample was *ca.* 3.5 nm, which was in agreement with pore size listed in Table 1.

4. Adsorption Capacity of CMK-3

4-1. Effect of pH on Cd(II) Ions Adsorption

The pH of adsorption medium plays an important role in investigating the adsorption capacity of the adsorbent. The effect of pH on the removal efficiency of Cd(II) ions on CMK-3 is shown in Fig. 4. It is evident that the initial pH significantly affected the adsorption capacity of CMK-3. The removal efficiency of Cd(II) ions on CMK-3 increased as the pH increased from 2 to 8. A similar trend was also observed in Ref. [35]. The pH corresponding to the deposition of $Cd(OH)_2$ was 8.8, calculated taking into account the Ksp (solubility product of $Cd(OH)_2$ (7.2×10^{-15}) and the initial concentration of Cd(II) ions (20 mg/L). Therefore, the pH above 8 was not investigated.

The effect of pH may be explained in terms of pH_{zpc} of the adsorbent. Fig. 5 shows the plot between pH_{final} versus $pH_{initial}$. The pH at which the curve crosses the $pH_{initial}=pH_{final}$ line was taken as pH_{zpc}. As shown in Fig. 5, pH_{zpc} of CMK-3 is 5.6, at which the adsorbent is neutral. This is similar to that of the Ref. [36]. The surface charge of the absorbent is positive when solution pH is below pH_{zpc} [37,38]; competition could occur between protons (H^+) and Cd(II) ions for available adsorption sites, which inhibits the adsorption of Cd(II) ions on CMK-3, resulting in the lower removal efficiency of Cd(II) ions. With the increasing of pH, the positive charge

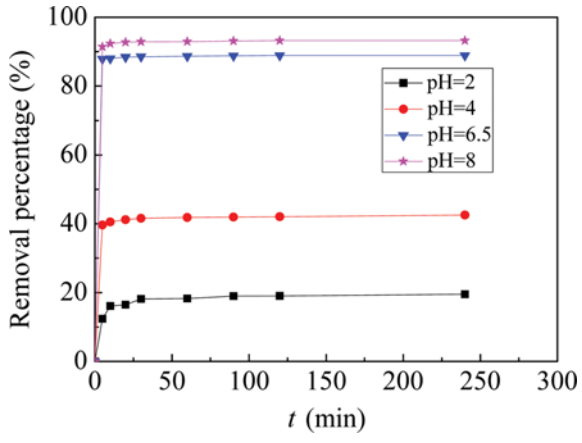

Fig. 4. Effect of pH on the removal percentage of Cd(II) ions onto CMK-3 (adsorbent dose=20 mg; $[Cd(II)]_{initial}$=20 mg/L; T=293 K; contact time=3 h).

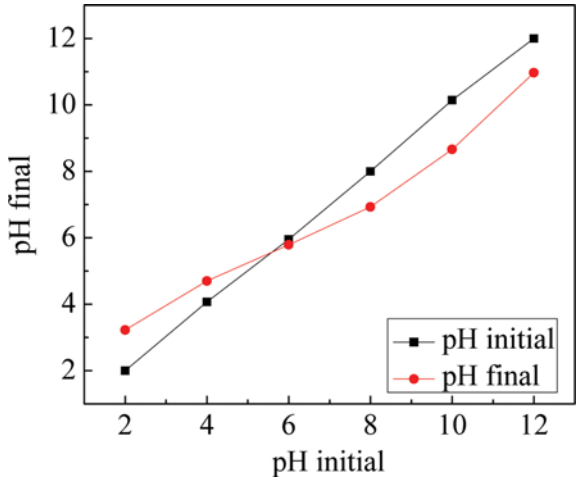

Fig. 5. The initial versus finial pH plot for determination of pH_{zpc} of CMK-3.

of the adsorbent surface decreases gradually. When solution pH is above pH_{zpc}, the surface of the CMK-3 is negative, and there is a strong electrostatic attraction between surface groups and Cd(II) species, resulting in the increase in the removal of Cd(II) ions.

4-2. Effect of Contact Time on Cd(II) Ions Adsorption

The effect of contact time on the removal of Cd(II) ions onto CMK-3 was investigated along with dose of 20 mg, initial Cd(II) ions concentration of 20 mg/L and pH 6.5 at ambient temperature. A series of adsorption experiments were carried out and the results are presented in Fig. 6. Obviously, the removal percentage of Cd(II) ions was quite fast initially and more than 87% of Cd(II) ions could be removed within 5 min. Then, the removal percentage increased slowly with the increase in contact time, reaching a plateau value after 20 min.

4-3. Effect of Temperature on Cd(II) Ions Adsorption

To investigate the effect of temperature on adsorption of Cd(II) ions, a series of experiments at 20, 30, 40 and 60 °C were performed and the results obtained are shown in Fig. 7. Note that the removal percentage of Cd(II) ions decreased slightly from 89.5 to 87% with the increase of temperature from 20 to 60 °C; a lower temperature is more favorable for the adsorption process, suggesting that the adsorption process is exothermic. This may be owing to the weaker attractive forces between the adsorbent and metal ions with increasing temperature [1]. Moreover, we observed from Fig. 7 that there was little difference between the removals in the temperature range from 20 to 60 °C; thus we selected 20 °C as the experimental temperature for further adsorption.

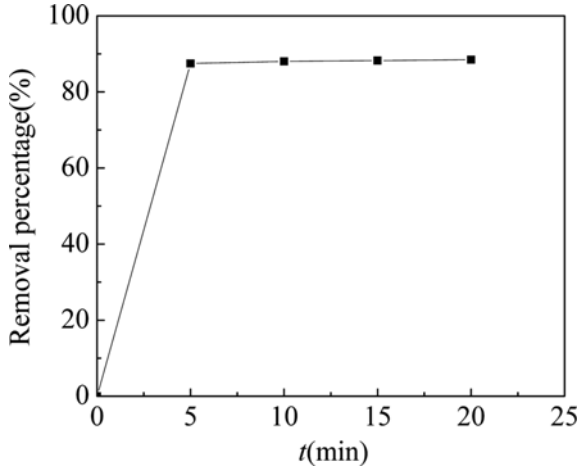

Fig. 6. Effect of contact time on the removal of Cd(II) ions onto CMK-3 (adsorbent dose=20 mg; pH=6.5; T=293 K; $[Cd(II)]_{initial}$ =20 mg/L).

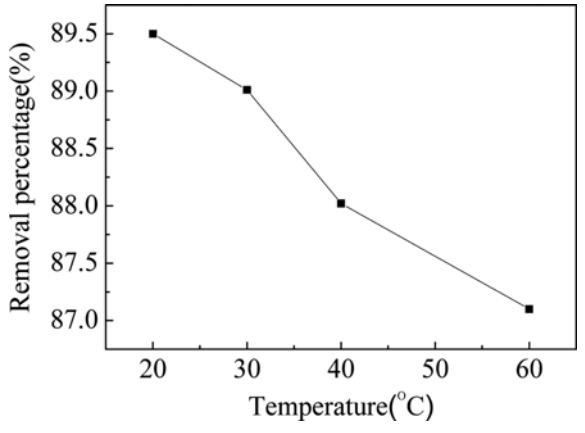

Fig. 7. Effect of temperature on the removal of Cd(II) ions onto CMK-3 (adsorbent dose=20 mg; pH=6.5; contact time=3 h; $[Cd(II)]_{initial}$=20 mg/L).

5. Adsorption Isotherm

Batch adsorption experiments were carried out to evaluate the adsorption capacity of CMK-3. Of which, 50 mL of Cd(II) ions solution with different initial concentrations from 8 to 20 mg/L was stirred at 293 K and the other parameters such as 20 mg adsorbents and the pH 6.5 were kept constant. The adsorption amount of CMK-3 versus the equilibrium concentration of Cd(II) ions in solution are plotted in Fig. 8. To indicate the adsorption behavior of Cd(II) ions on CMK-3, Langmuir and Freundlich isotherm models were used in the experiment. Langmuir isotherm model has been successfully used to characterize the monolayer adsorption process, and Freundlich isotherm model is derived by assuming adsorption on a heterogeneous surface. The linear plots obtained by Langmuir and Freundlich isotherm models are presented in Fig. 9(a) and (b). The adsorption data of Cd(II) ions were fitted by the Langmuir model with a correlation coefficient (R^2) of 0.99668. Also, we fitted the data with the Freundlich model (R^2=0.99239). The correlation coefficient (R^2) calculated from Langmuir model is higher than that of the Freundlich model. Therefore, the adsorption isotherm from Langmuir model is more satisfactory than that of Freundlich model, suggesting that the adsorption isotherm is a good fit with the Langmuir model and indicating that Cd(II) ions adsorption on CMK-3 is monolayer coverage. This result is in agreement with Ref. [39].

6. Kinetic of Adsorption

The linear plots of $\ln(q_e - q_t)$ versus t for the pseudo-first-order kinetic model and t/q_t versus t for the pseudo-second-order model for Cd(II) ions adsorption on CMK-3 are presented in Fig. 10(a)

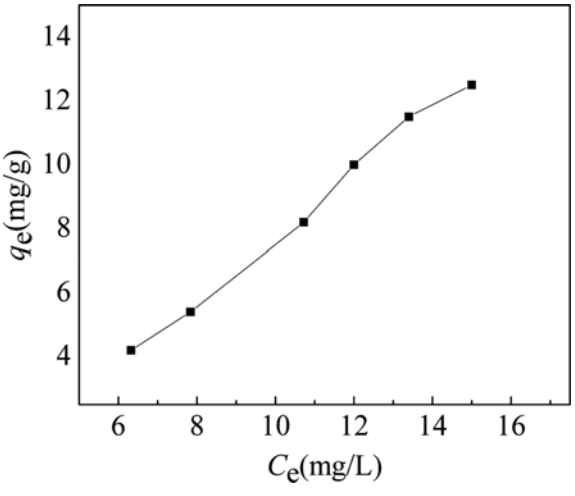

Fig. 8. Adsorption isotherm of Cd(II) ions onto CMK-3 at 298 K (adsorbent dose=20 mg; pH=6.5; $[Cd(II)]_{initial}$=8-20 mg/L; contact time=3 h).

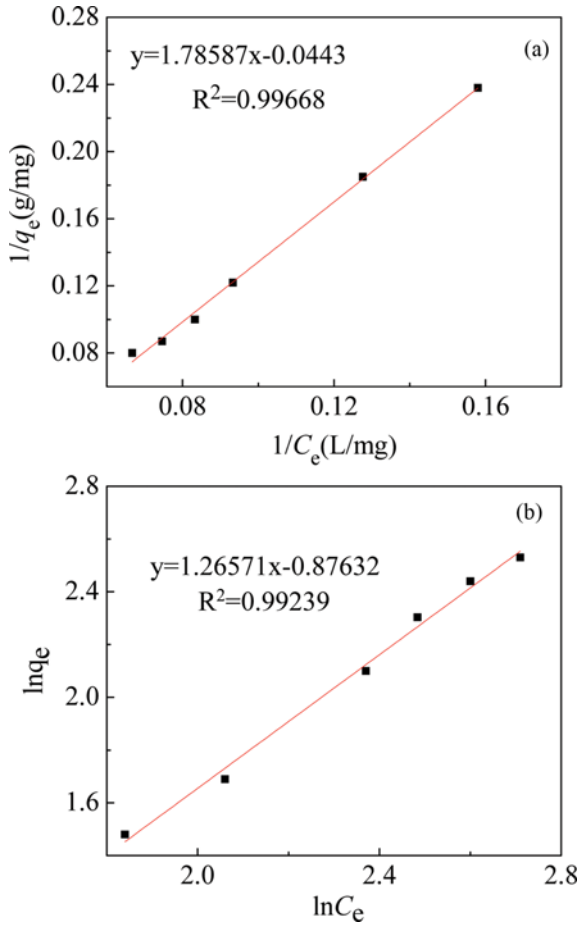

Fig. 9. The linear plots of Cd(II) ions adsorption onto CMK-3 at 293 K (a) Langmuir model and (b) Freundlich model.

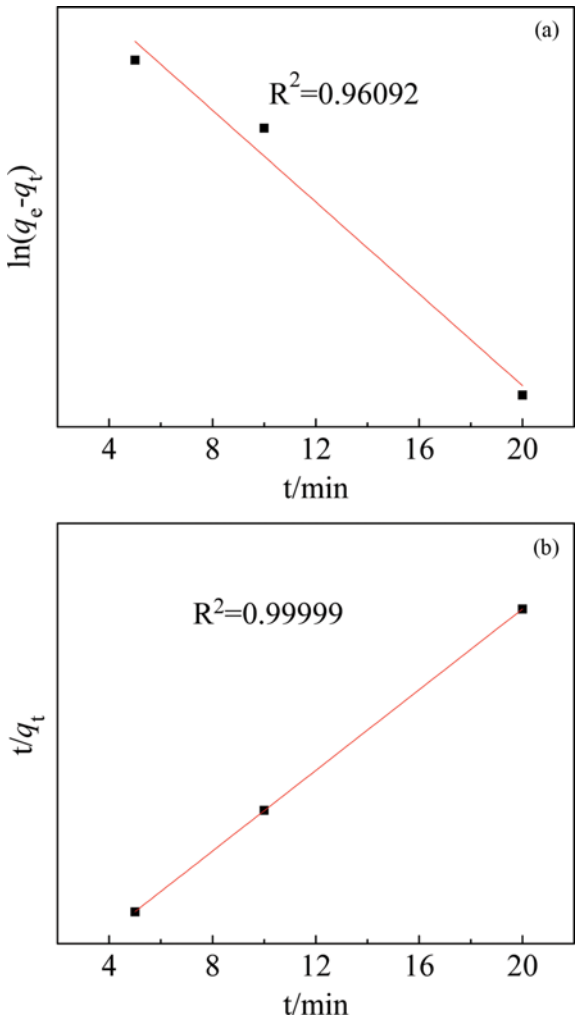

Fig. 10. Adsorption of Cd(II) ions on the CMK-3 composite (a) pseudo-first-order model and (b) pseudo-second-order model.

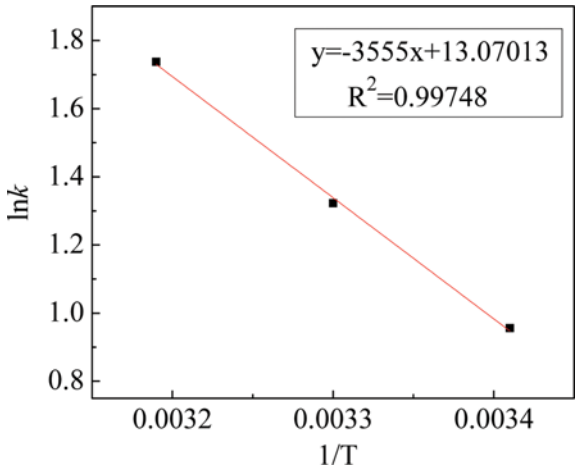

Fig. 11. The linear plot of ln*k* versus 1/T for Cd(II) ions adsorption on CMK-3 at 293, 303 and 313 K.

and (b). The pseudo-second-order kinetic model provided a good correlation coefficient (R^2=0.99999) for Cd(II) ions adsorption on CMK-3, suggesting that the pseudo-second-order kinetic model is able to describe properly the kinetic behavior of Cd(II) ions adsorption on CMK-3 and the Cd(II) ions uptake process is dominated by the chemical reaction. A similar result has been reported from Ref. [40].

Moreover, the rate constant k of the pseudo-second-order adsorption at 393, 303 and 313 K calculated by the pseudo-second-order equation (Eq. (6)) was 2.60, 3.43 and 5.68 g $mg^{-1}min^{-1}$, respectively. The linear plots of lnk versus 1/T for Cd(II) ions adsorption on CMK-3 at 293, 303 and 313 K are shown in Fig. 11. The activation energy (Ea) for adsorption system of Cd(II) ions on CMK-3 was calculated from the slope of the linear plot and the result obtained was 29.56 kJ/mol. According to Ref. [41], the rate is controlled by intra-particle diffusion mechanism; Ea value is low. Therefore, the adsorption process may be controlled by intra-particle diffusion, suggesting that is a physical step in the adsorption process. This result is similar to the Ref. [42].

CONCLUSIONS

Ordered mesoporous carbon (CMK-3) was synthesized using SBA-15 mesoporous molecular sieve as a template and sucrose as carbon source, and was characterized by means of XRD, TEM and

N_2 physical adsorption. The CMK-3 exhibited excellent adsorption efficiency for Cd(II) ions from aqueous solution. Under the optimum experimental conditions, the removal percentage for Cd(II) ions adsorption onto CMK-3 can achieve *ca.* 90%. The adsorption process of Cd(II) ions onto CMK-3 was found to follow the pseudo-second-order kinetic model and Langmuir isotherm model.

REFERENCES

1. H. Wang, X. Z. Yuan, Y. Wu, H. J. Huang, G. G. Zeng, Y. Liu, X. L. Wang, N. B. Lin and Y. Qi, *Appl. Surf. Sci.*, **279**, 432 (2013).
2. H. Sukpreabprom, O. Arqueropanyo, W. Naksata, P. Sooksamiti and S. Janhom, *Korean J. Chem. Eng.*, **32**, 896 (2015).
3. S. H. Khorzughy, T. Eslamkish, F. D. Ardejani and M. R. Heydartaemeh, *Korean J. Chem. Eng.*, **32**, 88 (2015).
4. F. Y. Wang, H. Wang and J. W. Ma, *J. Hazard. Mater.*, **177**, 300 (2010).
5. P. Ghosh, A. N. Samanta and S. Ray, *Desalination*, **266**, 213 (2011).
6. L. H. Liu, J. Wu, X. Li and Y. L. Ling, *Sep. Purif. Technol.*, **103**, 92 (2013).
7. A. Dbrowski, Z. Hubicki, P. Podkocielny and E. Robens, *Chemosphere*, **56**, 91 (2004).
8. M. Mohsen-Nia, P. Montazeri and H. Modarress, *Desalination*, **217**, 276 (2007).
9. M. E. Argun, S. Dursun, M. Karatas and M. Guru, *Bioresour. Technol.*, **99**, 8691 (2008).
10. T. Mohammadi, A. Moheb, M. Sadrzadeh and A. Razmi, *Sep. Purif. Technol.*, **41**, 73 (2005).
11. F. P. Zhao, E. Repo, D. L. Yin and M. E. T. Sillanpää, *J. Colloid Interface Sci.*, **409**, 174 (2013).
12. S. P. Chen, J. X. Hong, H. X. Yang and J. Z. Yang, *J. Environ. Radioact.*, **126**, 253 (2013).
13. Z. Huang, X. Zheng, W. Lv, M. Wang, Q. Yang and F. Kang, *Langmuir*, **27**, 7558 (2011).
14. S. G. Liu, Y. Q. Ding, P. F. Li, K. S. Diao, X. C. Tan, F. H. Lei, Y. H. Zhan, Q. M. Li, B. Huang and Z. Y. Huang, *Chem. Eng. J.*, **248**, 135 (2014).
15. P. Xu, G. M. Zeng, D. L. Huang, C. L. Feng, S. Hu, M. H. Zhao, C. Lai, Z. Wei, C. Huang, G. X. Xie and Z. F. Liu, *Sci. Total Environ.*, **424**, 1 (2012).
16. J. Hu, M. C. Lo and G. H. Chen, *Water Sci. Technol.*, **50**, 139 (2004).
17. G. Zhao, J. Li, X. Ren, C. Chen and X. Wang, *Environ. Sci. Technol.*, **45**, 10454 (2011).
18. V. C. Srivastava, I. D. Mall and I. M. Mishra, *Chem. Eng. Process.*, **47**, 1269 (2008).
19. S. Kumar, V. A. Loganathan, R. B. Gupta and M. O. Barnett, *J. Environ. Manage.*, **92**, 2504 (2011).
20. W. J. Yang, P. Ding, L. Zhou, J. G. Yu, X. Q. Chen and F. P. Jiao, *Appl. Surf. Sci.*, **282**, 38 (2013).
21. M. F. R. Pereira, S. F. Soares, J. J. M. Orfao and J. L. Figuerredo, *Carbon*, **41**, 811 (2003).
22. V. Gómez, M. S. Larrechi and M. P. Calla, *Chemosphere*, **69**, 1151 (2007).
23. J. Avom, J. K. Mbadcam, C. Noubactep and P. Germain, *Carbon*, **35**, 365 (1997).
24. Z. G. Jia, Q. Z. Wang, D. P. Ren and R. S. Zhu, *Appl. Surf. Sci.*, **264**, 255 (2013).
25. R. Ryoo, S. H. Joo and S. Jun, *J. Phys. Chem. B*, **103**, 7743 (1999).
26. J. Goscianska, A. Olejinik and R. Pietrzak, *J. Taiwan Inst. Chem. Eng.*, **45**, 347 (2014).
27. Y. Tian, P. Liu, X. Wang and H. Lin, *Chem. Eng. J.*, **171**, 1263 (2011).
28. A. Vinu, M. Miyahara, V. Sivamurugan, T. Mori and K. Ariga, *J. Mater. Chem.*, **155**, 122 (2005).
29. D. Y. Zhao, Q. S. Huo, J. L. Feng, B. F. Chmelka and G. D. Stucky, *J. Am. Chem. Soc.*, **120**, 6024 (1998).
30. S. Jun, S. H. Joo, R. Ryoo, M. Kruk, M. Jaroniec, Z. Liu, T. Ohsuna and O. Terasaki, *J. Am. Chem. Soc.*, **122**, 10712 (2000).
31. R. Ahmad, R. Kumar and S. Haseeb, *Arabian J. Chem.*, **5**, 353 (2012).
32. D. Zhao, J. Feng, Q. Huo, N. Melosh, G. H. Fredrickson, B. F. Chmelka and G. D. Stucky, *Science*, **279**, 548 (1998).
33. L. F. Wang, S. Lin, K. F. Lin, C. Y. Yin, D. S. Liang, Y. Di, P. W. Fan, D. Z. Jiang and F. S. Xiao, *Micropor. Mesopor. Mater.*, **85**, 136 (2005).
34. C. T. Kresge, M. E. Leonowicz, W. J. Roth, J. C. Vartuli and J. S. Beck, *Nature*, **359**, 710 (1992).
35. H. P. Ye, Q. Zhu and D. Y. Du, *Bioresour. Technol.*, **101**, 5175 (2010).
36. M. J. Baniamerian, S. E. Moradi, A. Noori and H. Salahi, *Appl. Surf. Sci.*, **256**, 1347 (2009).
37. Y. C. Sharma, Uma and S. N. Upadhyay, *Energy Fuels*, **23**, 2983 (2009).
38. B. Al-Rashdi, C. Tizaoui and N. Hilal, *Chem. Eng. J.*, **183**, 294 (2012).
39. Y. J. Tu, C. F. You and C. K. Chang, *J. Hazard. Mater.*, **235-236**, 116 (2012).
40. P. Xu, G. M. Zeng, D. L. Huang, C. Lai, M. H. Zhao, Z. Wei, N. J. Li, C. Huang and G. X. Xie, *Chem. Eng. J.*, **203**, 423 (2012).
41. M. Doğan and M. Alkan, *Chemosphere*, **50**, 517 (2003).
42. I. Mobasherpour, E. Salahi and M. Ebrahimi, *J. Saudi Chem. Soc.*, **18**, 792 (2014).